Géographie physique et Quaternaire

Emergence and Migration of a Nearshore Bar: Sediment Flux and Morphological Change on a Multi-Barred Beach in the Great Lakes

Brian Greenwood, Allana Permanand-Schwartz et Christopher A. Houser

Volume 60, numéro 1, 2006

URI : https://id.erudit.org/iderudit/016363ar
DOI : https://doi.org/10.7202/016363ar

Aller au sommaire du numéro

Éditeur(s)

Les Presses de l'Université de Montréal

ISSN

0705-7199 (imprimé)
1492-143X (numérique)

Découvrir la revue

Citer cet article

Greenwood, B., Permanand-Schwartz, A. & Houser, C. A. (2006). Emergence and Migration of a Nearshore Bar: Sediment Flux and Morphological Change on a Multi-Barred Beach in the Great Lakes. *Géographie physique et Quaternaire*, *60*(1), 31–47. https://doi.org/10.7202/016363ar

Résumé de l'article

Émersion et migration d'une barre côtière : bilan sédimentaire et changements morphologiques d'une plage à barres multiples des Grands Lacs. La plage de Burley (sud-est du lac Huron) présente une avant-côte à barres multiples, état morphologique caractéristique de l'équilibre à long terme des plages sableuses à pente faible. Au cours d'un seul orage majeur, une nouvelle barre s'est développée à 50-60 m au large de la côte en forme de creux et crête irrégulière, suite à l'érosion d'une terrasse côtière. L'émersion, la croissance et la migration de la barre est attribuable à (a) un bilan sédimentaire négatif dans la zone interne du ressac (-2,30 m^3/m), mais à un bilan sédimentaire positif (+5,10 m^3/m) durant l'apogée et la dissipation de l'orage, (b) l'exondation du gradin de plage pour générer une nouvelle terrasse côtière et (c) la migration de deux barres distales au large de la côte, laissant assez d'espace pour la mise en place d'une nouvelle barre. Les mécanismes de l'émersion, de la croissance et de la migration sont : (a) les contre-courants qui transportent les sédiments en suspension au large de la côte et (b) le transport vers la côte via la fréquence des vagues de gravité générées au début de l'orage et par les vagues d'infragravité subséquentes (au maximum de l'orage et durant sa dissipation). Le transport brut des sédiments est important, mais le résultat net correspond seulement à un léger transport vers le sud-ouest (direction historique du transit littoral). Ceci ne cause pas la création de la barre, mais peut contribuer aux apports sédimentaires nécessaires à sa croissance. Le mécanisme responsable de l'évolution des barres est le transport des sédiments par les vagues oscillatoires et les contre-courants.

Géographie physique et Quaternaire, 2006, vol. 60, nº 1, p. 31-47, 15 fig., 1 tabl.

EMERGENCE AND MIGRATION OF A NEARSHORE BAR: SEDIMENT FLUX AND MORPHOLOGICAL CHANGE ON A MULTI-BARRED BEACH IN THE GREAT LAKES

Brian GREENWOOD*, Allana PERMANAND-SCHWARTZ and Christopher A. HOUSER; first author: Scarborough College Coastal Research Group, Department of Physical and Environmental Sciences, University of Toronto, Scarborough, 1265 Military Trail, Toronto, Ontario M1C 1A4, Canada; second author: University of New Brunswick, P.O. Box 4400, Fredericton, New Brunswick E3B 5A3, Canada; third author: Department of Environmental Studies, University of West Florida, 11000 University Parkway, Pensacola, Florida 32514-5750, United States.

ABSTRACT Burley Beach (southeastern Lake Huron) exhibits a multi-barred shoreface, the long-term equilibrium morphology characteristic of many low angle, sandy beaches in the Canadian Great Lakes. During a single major storm, a new bar emerged 50-60 m offshore as an irregular trough-crest form, through differential erosion of an existing shore terrace. Emergence, bar growth and offshore migration were associated with: (a) an overall negative sediment balance in the inner surf zone initially (-2.30 m^3/m beach width), but with a large positive sediment balance (+5.10 m^3/m) subsequent to the storm peak and during the storm decay; (b) progradation of the beach step to produce a new shore terrace; and (c) offshore migration of the two outer bars to provide the accommodation space necessary for the new bar. The primary transport mechanisms accounting for emergence of the new bar, its growth and migration were: (a) the mean cross-shore currents (undertow), which always transported suspended sediment offshore; and (b) the onshore transport of suspended sediment by incident gravity wave frequencies early in the storm and subsequently by infragravity waves (at the storm peak and the decay period). The longshore transport of sediment was significant in terms of the gross transport, although the net result was only a small transport to the south-west (historic littoral transport direction). It did not cause bar initiation, but it may have supplied some of the sediment for bar growth. The primary mechanism for bar initiation and growth was the cross-shore displacement of sediment by wave-driven (oscillatory) transport and cross-shore mean currents (undertow).

RÉSUMÉ *Émersion et migration d'une barre côtière : bilan sédimentaire et changements morphologiques d'une plage à barres multiples des Grands Lacs.* La plage de Burley (sud-est du lac Huron) présente une avant-côte à barres multiples, état morphologique caractéristique de l'équilibre à long terme des plages sableuses à pente faible. Au cours d'un seul orage majeur, une nouvelle barre s'est développée à 50-60 m au large de la côte en forme de creux et crête irrégulière, suite à l'érosion d'une terrasse côtière. L'émersion, la croissance et la migration de la barre est attribuable à (a) un bilan sédimentaire négatif dans la zone interne du ressac (-2,30 m^3/m), mais à un bilan sédimentaire positif (+5,10 m^3/m) durant l'apogée et la dissipation de l'orage, (b) l'exondation du gradin de plage pour générer une nouvelle terrasse côtière et (c) la migration de deux barres distales au large de la côte, laissant assez d'espace pour la mise en place d'une nouvelle barre. Les mécanismes de l'émersion, de la croissance et de la migration sont : (a) les contre-courants qui transportent les sédiments en suspension au large de la côte et (b) le transport vers la côte via la fréquence des vagues de gravité générées au début de l'orage et par les vagues d'infragravité subséquentes (au maximum de l'orage et durant sa dissipation). Le transport brut des sédiments est important, mais le résultat net correspond seulement à un léger transport vers le sud-ouest (direction historique du transit littoral). Ceci ne cause pas la création de la barre, mais peut contribuer aux apports sédimentaires nécessaires à sa croissance. Le mécanisme responsable de l'évolution des barres est le transport des sédiments par les vagues oscillatoires et les contre-courants.

Manuscrit reçu le 30 janvier 2006 ; manuscrit révisé accepté le 12 octobre 2006 (publié le 2e trimestre 2007)
* E-mail address: greenw@utsc.utoronto.ca

INTRODUCTION

Wave-formed or nearshore bars were recognized in the Great Lakes of North America as early as the mid-1800s (Desor, 1851; Andrews, 1870; Whittlesey, 1896). Evans (1940) termed such features in Lake Michigan, "balls" and "lows", and reviewed much of the earlier literature on such features in other large lakes (Gilbert, 1885; Russell, 1885). He concluded that the lows and balls were associated with plunging breakers in a manner similar to that later described from laboratory experiments by Keulegan (1948), Miller (1976) and others. The terms "ridge" and "trough" had been used earlier by Kindle (1936), while the terms "bar" and "trough" became entrenched in the literature with the classic work of Shepard (1950). Bar-trough systems are ubiquitous features on low-angle, sandy shorefaces throughout the Great Lakes (Saylor and Hands, 1970; Davis and Fox, 1972a, 1972b; Gillie, 1974; Hands, 1976; Davidson-Arnott and McDonald, 1980; Greenwood, 1987; Davidson-Arnott, 1988), in other large lakes worldwide (Keranen, 1985) and on marine coasts in Canada (Greenwood and Davidson-Arnott, 1975, 1979; Owens, 1977; Greenwood and Mittler, 1979, 1984; Hale and McCann, 1982) and elsewhere in the world (Zenkovitch, 1967; King, 1972; Carter, 1988; Greenwood, 2003, 2004).

The association between bar-trough profiles and storm-wave activity is well established, but the transition from barred to non-barred profiles at different seasons (Inman *et al.*, 1993) is not seen in the Great Lakes, although beach profiles are displaced seasonally in association with changing lake levels (Dubois, 1973). Barred and non-barred profiles do not generally co-exist at the same site in the Great Lakes, nor are they part of a morphodynamic sequence as proposed by Wright *et al.* (1979), Wright and Short (1984) and Lippman and Holman (1990). The relaxation time between the forcing conditions and bar-trough adjustment is relatively short in the Great Lakes, since the relief is relatively small and the fetch-restricted environments produce rapid growth and decay of storm waves; however, there is no sustained post-storm swell. In the short term, individual bar-trough systems are almost always in a transient state, although in the long term (years-to-decades), a barred profile can be thought to represent the equilibrium morphology for virtually all sandy nearshore environments in the Great Lakes.

Although there are a significant number of different explanations both for the origins and dynamics of bars (see Wijnberg and Kroon, 2002; Greenwood, 2003, 2004 for recent reviews), our knowledge of bar morphodynamics is far from complete, with "unexpected" bar behaviour appearing frequently (Lippmann *et al.*, 1993; Aagaard and Greenwood, 1999; Southgate and Möller, 2000). As with all topographic forms, changes are dictated by spatial and temporal gradients in the local sediment flux. Such gradients are not predictable at present, and field experiments are necessary to limit the large number of possible transport processes, rates and gradients. Our understanding of bars is particularly restricted by the fact that the initial stages of bar-trough evolution from a plane bed have rarely been recorded in the field, especially where the associated sediment flux and its forcing have also been recorded (see Thornton *et al.*, 1996). In this paper, we focus on topographic changes that occurred during a complex, single storm event in the Great Lakes as a "new" bar emerged and migrated lakeward. The local forcing and resultant suspended sediment transport (both direction and magnitude) will be used to explain the link between sediment flux and bar evolution.

STUDY SITE

LOCATION AND MORPHOLOGY

Burley Beach, located within Pinery Provincial Park on the southeastern shore of Lake Huron, Ontario, Canada (81° 53' 27" W, 43° 14' 23" N; Fig. 1), is composed primarily of sand (mean grain size of 180-200 µm), with an admixture of gravel in distinct layers. It is part of the terminal sink for a littoral cell stretching from Clark Point in the north to a down drift boundary at Kettle Point (Fig. 1). Sediment accumulation to the north of Kettle Point over the last 6000 years has resulted in the infilling of a large Lake Algonquin-Nippising embayment (the Thedford embayment; Cooper, 1976) and progradation of a large dune system. The barred shoreface at Burley has therefore evolved in an area of a positive net sediment budget, at least in the long term.

FIGURE 1. Location of study site, Burley Beach, Lake Huron, Ontario at 81° 53' 27" W, 43° 14' 23" N. Note the location of the United States National Oceanographic and Atmospheric Administration (NOAA) wave rider buoy 45008 at 82° 23' 59" W, 44° 18' 00" N.

Localisation du site d'étude, plage de Burley, lac Huron, Ontario à 81° 53' 27" W, 43° 14' 23" N. Notez l'emplacement de la bouée 45008 du United States National Oceanographic and Atmospheric Administration *(NOAA) à 82° 23' 59" W, 44° 18' 00" N.*

The upper-shoreface slopes at ~0.009 and is characterised by 2-3 quasi-permanent bars; the beach face is steeper and characterized by an ephemeral swash ridge or berm (Fig. 2). The outer and middle bars (Bars 3 and 2 respectively*)* are quasi-linear in plan form, while the inner bar (Bar 1) and the swash ridge may be significantly more three-dimensional, but only rarely segmented by rip channels (Fig. 3). Prior to the experiment, profiles were constructed at intervals of 35 m, for a distance of 1 100 m alongshore in order to identify the 3-dimensional nature of the bars. Although Bars 1 and 2 exhibit some degree of plan form sinuosity, it was small and certainly not periodic. The nearshore bathymetry is therefore predominantly two-dimensional (Fig. 3). The average spacing between the crests and between the troughs of Bars 1 and 2 in the alongshore direction is respectively 43 m (standard deviation of ±10.0 m) and 42 m (standard deviation of ±9.5 m). The swash ridge and Bar 1 are subject to a much wider range of breaking wave conditions, as well as disruption by the ice foot during the winter, than the other bars; they are therefore much more variable in both form and location and, at times, Bar 1 is replaced by a shallow shore terrace (Fig. 1).

Gillie (1980) showed that the cross-shore location of Bars 2 and 3 were relatively stable, each simply oscillating about a mean position, while Bar 1 was much more dynamic. Houser and Greenwood (2005) proposed that the bar system was subject to a longer period cyclic behaviour, with the position and spacing of the inner bars subject to a "self-organized equilibrium" in the shorter term, constrained by wave breaking on the outermost bar, Bar 3. However, as the latter moves offshore, it shifts lower on the profile and degrades (see Wijnberg, 1995; Ruessink and Terwindt, 2000; Shand, 2003; Houser and Greenwood, 2005), which allows a new wave regime to penetrate the inner system during storms, causing a rapid bar migration lakeward to re-establish Bar 3, and a new bar is initiated at the shoreline, moving rapidly to relatively fixed position offshore in a manner similar to that proposed for marine bars by Ruessink and Terwindt (2000). In this paper, the dynamics of the innermost bar, Bar 1, are explored and its emergence and migration are examined, together with the sediment flux that controls this behaviour.

LAKE HURON WATER LEVELS

Water levels are critical to the dynamics of the nearshore zone and they vary at a wide range of temporal scales. The seasonal and long-term levels are controlled primarily by the hydrologic balance within the Great Lakes' basin; historically, the difference between the lowest and highest levels is 1.9 m. However, such variation can occur over much shorter periods in association with individual storm surges, and even lake seiches cause level changes of +0.25 m over a period of hours. It is these last two changes in water levels that constrain the inshore wave climate and thus the processes that control the short-term dynamics of bars.

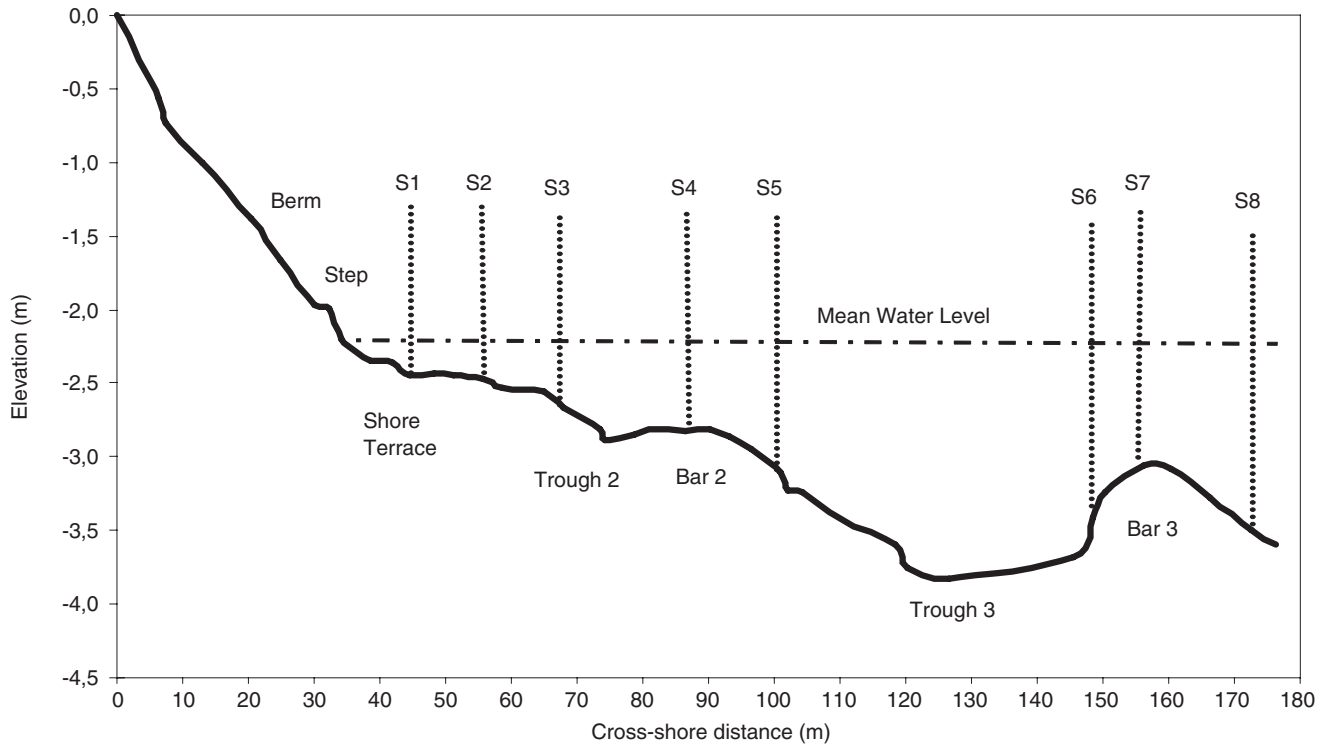

FIGURE 2. Nearshore topographic profile along the instrumented transect T3 at Burley Beach on October 9th, 2001. The beach morphology and the location of the bars and troughs are shown, as are the sediment transport stations.

Profil topographique de la côte le long du transect T3 à la plage de Burley, le 9 octobre 2001. La morphologie de la plage et la localisation des barres et des dépressions sont illustrées, de même que les stations de mesure du transport des sédiments.

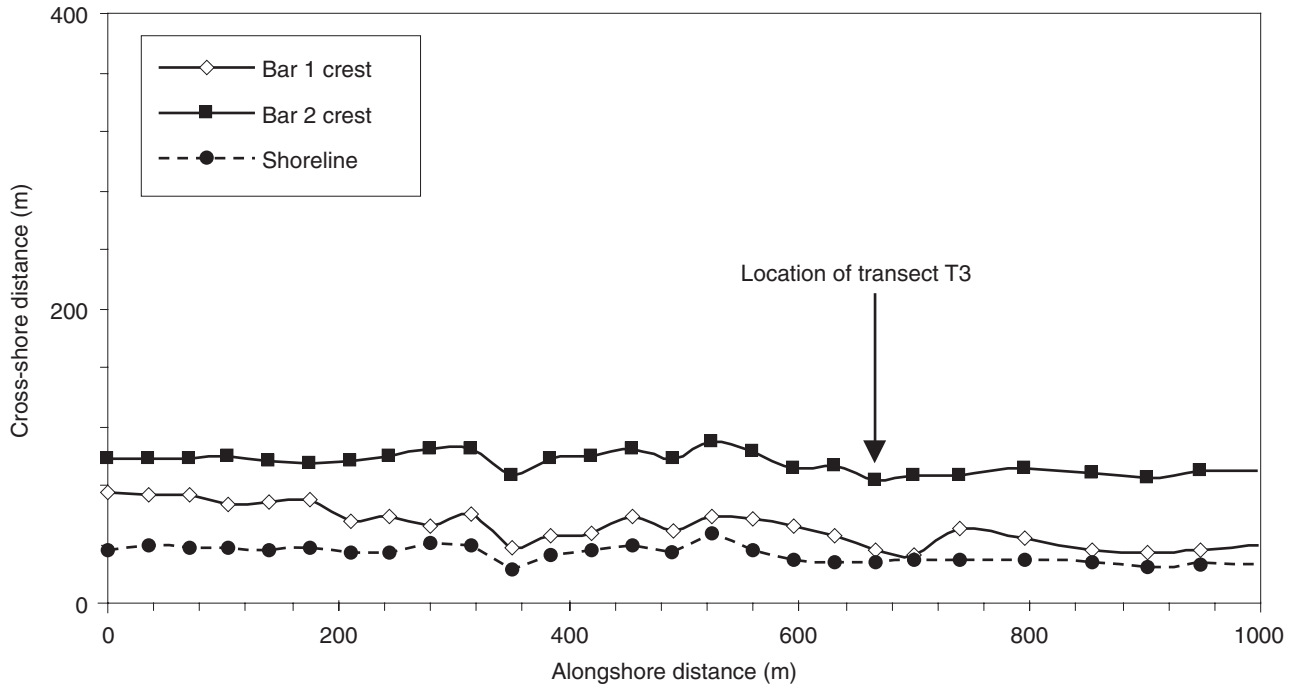

FIGURE 3. Alongshore pattern exhibited by the shoreline and the two innermost bar crests, as well as the intervening troughs at Burley Beach; the location of the instrumented transect T3 is also shown. The surveys were carried out over a few days of flat calm weather in the summer of 2001.

Patron du littoral montrant la ligne de rivage, les deux barres internes et les crêtes à la plage de Burley ; l'emplacement du transect T3 est également illustré. Les levés ont été effectués durant les rares jours de conditions météorologiques calmes de l'été 2001.

WIND AND WAVE CLIMATE

Burley Beach is exposed to a very restricted fetch and as a result the wave climate is dominated by local, storm-generated, wind-waves propagating through a window from the NW through SW quadrants; maximum fetch is to the NNW and is 300 km. While waves are often more regular in the immediate post-storm conditions, there is no true swell. Deep-water wave heights can exceed 5 m during large storms, with peak periods of 9-11 s (Buoy 45008 located at 82° 23' 59" W, 44° 18' 00" N; National Data Buoy Centre, available online at http://mob.ndbc.noaa.gov/; Fig. 1). Extreme value analysis of measurements since 1981 indicates that waves of this magnitude have a return period of 11 years (Houser, 2004). The mean annual deepwater significant wave height is 2.0 m, with wave periods of 4-6 s. Storms can occur at anytime of the year and the inshore (8 m water depth) spectral characteristics reveal that most of the wave energy is rather narrowly focused around 0.07 Hz and the directional spread is relatively small. However, high-energy events are most frequent during the autumn and winter, coincident with a change in atmospheric circulation and the southerly tracking of frontal systems across the Great Lakes (Angel and Isard, 1997; Isard *et al.*, 2000). In fall, the mean monthly deepwater wave height is 1.0 m (September to December), while in summer (May to August) it is only 0.4 m.

EXPERIMENTAL METHODS

MORPHOLOGY AND MORPHOLOGICAL CHANGE

Changes in the form and location of the nearshore bars were determined, from topographic profiles using standard levelling techniques, and repeated frequently throughout the experimental period along a single transect (T3). This transect was also used to deploy the instrumentation. Surveys were conducted perpendicular to the shoreline from a datum at the base of the foredune (in this paper all distances will be referenced to this point). The profiles were extended at least to the lakeward slope of the outermost bar (Bar 3). Differences between surveys record the net change in sediment volumes as well as areas of erosion and accretion; the volumetric change was recorded as m^3/m of shoreline.

WAVES, CURRENTS AND SEDIMENT FLUX

Instruments to record the local hydrodynamics and suspended sediment transport (SST) were deployed at eight stations along transect T3. Each station was equipped with a strain gauge pressure transducer (VIATRAN 2406AEG) to record the instantaneous (waves) and average (set up) water elevations. Two components of the near-bed horizontal velocity field were recorded with bi-directional electromagnetic current meters (Marsh-McBirney OEM523 and OEM512) placed at nominal elevations of z = 0.05 and 0.15 m. The near-bed vertical structure of the sediment concentration was recorded with an array of three optical backscatter suspended solids sensors (Model OBS-1P, D & A Instrument Company); these sensors were placed nominally at z = 0.05, 0.10 and 0.15 m. It was not possible to adjust instrument elevations during storm; however, the exact elevations were recorded, and the instruments adjusted to their nominal elevations, whenever a topographic survey was carried out. The eight stations (S1-S8)

were deployed at intervals of 15 m from the shoreline out to a distance of 120 m (Fig. 2), and the sensors were all hardwired ashore. Although devices for measuring bedload transport rates under waves in the field have been proposed (Lowe, 1989), to date none have been completely successful; other studies have shown that SST is dominant in the surf zone (Sternberg *et al.*, 1989).

DATA ACQUISITION AND DATA ANALYSIS

Data were recorded using a shore-based acquisition system (Personal DAQ 56), consisting of a notebook computer-controlled high speed multiplexer and voltmeter. During the experiment, sensors were sampled at 4 Hz for a burst period of 45 minutes approximately every hour. Spectral and cross-spectral analyses, as well as other statistical computations, were carried out using Statistica™; individual data sets contained 10 900 values. Records from station S2 at 60 m, S4 at 94 m and S8 at 172 m from the baseline will be the focus for analyses in this paper.

SUSPENDED SEDIMENT TRANSPORT CALCULATIONS

Times series of the collocated, instantaneous velocities and suspended sediment concentrations were used to compute the time-averaged net, $<q_s>_{net}$, mean, $<q_s>_{mean}$ and oscillatory $<q_s>_{osc}$ components of the suspended sediment transport rate:

$$< q_s >_{net} = \frac{1}{T}\int_0^T \int_0^h U_{(z,t)} \; C_{(z,t)} \; dzdt$$

$$< q_s >_{mean} = \frac{1}{T}\left[\int_0^T \int_0^h U_{(z,t)} dzdt\right] * \frac{1}{T}\left[\int_0^T \int_0^h C_{(z,t)} dzdt\right]$$

$$< q_s >_{osc} = \frac{\Delta f}{F}\int_0^T \int_0^h C_{UC(f)} dzdt$$

where U = instantaneous velocity, which can be disaggregated into a cross-shore and alongshore components; C = instantaneous sediment concentration; z = elevation; t = time; $C_{UC(f)}$ = cospectrum of U and C; Δf = unit bandwidth; F = frequency range; h = water depth; and T = time. The cospectrum is the real part of a cross-spectral analysis, and allows the oscillatory transport to be subdivided by frequency. Transport by gravity and infragravity waves was separated at a frequency of 0.05 Hz, which is a conservative lower frequency limit for incident gravity waves in this fetch-limited environment; pronounced reductions in variance around this frequency in both wave and current spectra support this division.

STORM EVENT: OCTOBER 14TH-18TH, 2001

WINDS, WAVES AND CURRENTS

Winds and wind-forced waves were generated by the passage of a rather complex meteorological system, which produced two distinct wave regimes. From October 14th, 11:05 until October 16th, 07:00, wind speeds did not exceed 10 m/s, but the direction remained relatively steady around 240° (WSW; Fig. 4A). As a result, wave heights did increase (Fig. 4B), but breaking was restricted to the inner nearshore, *i.e.* landward of station S6 (Fig. 5). While the inner surf zone was only fully saturated for a matter of a few hours, breaking of the highest waves extended periodically lakeward of the second bar for a period of 36 h in total (12:00 on October 14th to 03:00 on the 16th).

However, in the early evening of the 16th, a rapidly moving cold front caused winds to switch to the NNW (virtually normal to the shoreline orientation) and to increase in speed up to 18 m/s (Fig. 4A). Incident wave height responded dramatically, increasing by 1 m within 4 h, (19:15-00:00; Fig. 4B) at the outer limit of the surf zone (station S8). Maximum significant height and peak period (H_s = 1.44 m, T_{pk} = 6.8 s) were recorded just before midnight on the 16th, with wave saturation occurring at station S8 for 14 h (Fig. 5). It was at this time, that significant surging across the beach face and backshore reached the base of the sand dunes, 30 m from the still water line and 1.5 m above the still water level. After 09:00, October 17th, there was a relatively rapid decrease in wind speed from 12 to 3.5 m/s, and winds shifted to the southeast and south. This was coincident with a gradual decrease in wave height at station S8, inducing shoaling rather than breaking, while wave breaking continued in the inner nearshore until around 07:30 on the 18th of October.

The maximum orbital velocities recorded at station S2 were simply a direct reflection of the changes in wave height (compare Fig. 5 and 6A); for example, the maximum significant wave height at this station was 1.33 m, which coincided with the maximum u_m of 1.68 m/s. Throughout the event, the cross-shore oscillatory velocity skewness was positive (shoreward directed; Fig. 6A), while the mean cross-shore currents were consistently directed offshore, but varied in speed ranging up to -0.30 m/s (Fig. 6B). The longshore currents were even larger ranging up to 0.50 m/s, although the direction was variable reflecting the variable wind and wave direction (Fig. 6B). The strongest current was directed to the NE at 19:15 on October 14th, when the winds were out of the W to WSW at speeds of 5.28 m/s. The current decreased and switched to the southwest as the wind shifted towards the east and north (Fig. 4A). This south-westerly flow attained maximum velocities of 0.44 m/s during the last 9 hours of the storm. At the storm peak, the longshore current reached a minimum (-0.06 m/s), reflecting the switch in wind direction from the SE to the NW. In comparison, the cross-shore mean currents attained velocities of 0.22 m/s (Fig. 6B).

Considerable attention has been paid in the literature over the last two decades to the form and origin of waves with frequencies outside the incident gravity band; measurements at Burley Beach also reveal significant infragravity and far infragravity motions in the surf zone, especially as the second phase of the storm evolved. Statistically significant spectral peaks were identified in the cross-shore velocity spectrum at station S2 at infragravity frequencies 0.014 Hz (70 s) and 0.049 Hz (20 s) and far infragravity frequencies 0.006 Hz (333 s or 5.5 minutes).

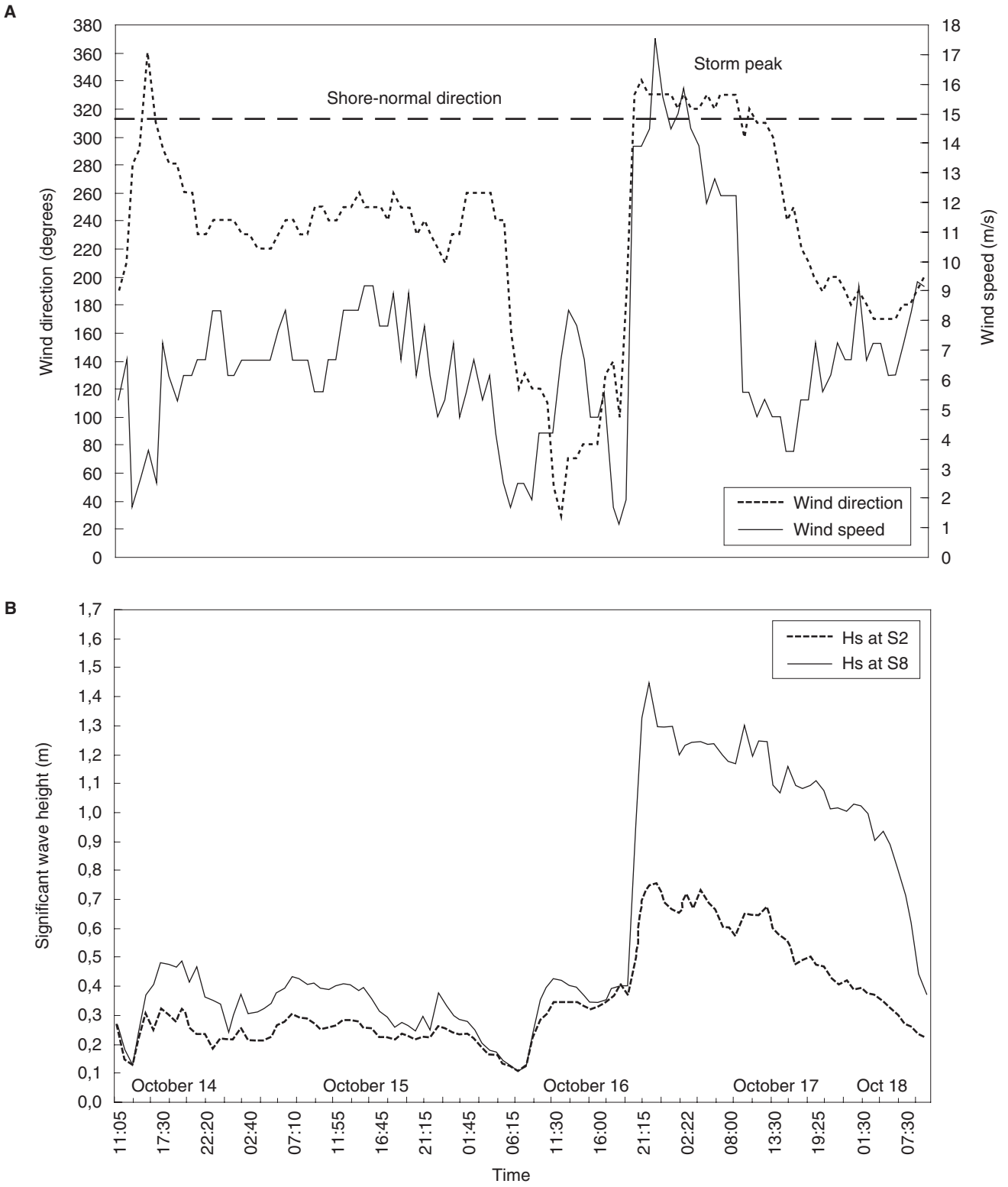

FIGURE 4. Time series of (A) wind speed and direction generated by a complex meteorological depression that moved through the area between October 14th and 18th, 2001; and (B) significant wave height recorded at stations S2 and S8. Note the rapid change in speed and direction on October 16th associated with the intense low-pressure cell and the dramatic shift in wave conditions.

Séries temporelles de (A) la vitesse et de la direction des vents générés par une dépression météorologique complexe qui a survolé la région entre le 12 et le 18 octobre 2001, et de (B) la hauteur des vagues significatives enregistrées aux stations S2 et S8. Notez les changements rapides de vitesse et de direction le 16 octobre, associés au passage de la cellule de basse pression intense et le changement drastique dans les conditions des vagues.

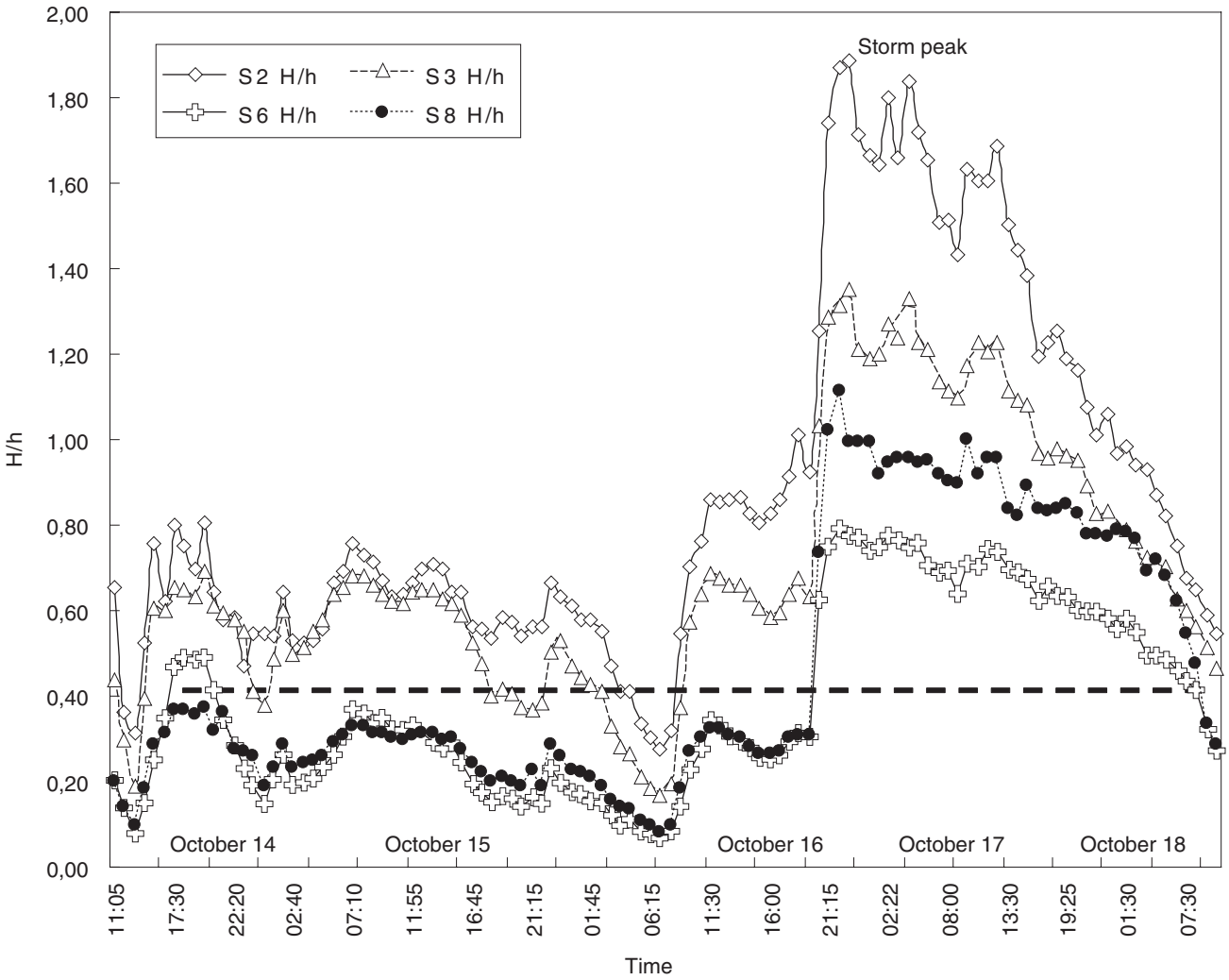

FIGURE 5. Time series of relative wave height (H/h, where H = wave height and h = local water depth at each station) measured at stations S2, S3, S6 and S8. Note: a reasonable value for the H_b / h ratio for wave breaking in this environment is 0.4 and this is shown on the graph by the horizontal dashed line.

Séries temporelles de la hauteur relative des vagues (H/h, où H = hauteur des vagues et h = profondeur d'eau locale à chaque station) mesurée aux stations S2, S3, S6 et S8. Note : la valeur du ratio H_b / h permettant la cassure des vagues est de 0,4 pour cet environnement, et elle est représentée sur le graphique par une ligne horizontale en tireté.

SEDIMENT BALANCE AND MORPHODYNAMIC RESPONSE

Three topographic surveys recorded the response of the upper shoreface morphology and the local sediment balance to the storm event: one survey prior to any significant wave activity (October 9th), one after the complete event (October 18th), and one, restricted to the inner surf zone, midway through the event during a "relatively" calm period prior to the passage of the intense low-pressure cell (October 16th). Wave breaking was essentially confined to the inner nearshore (out to 90 m) between October 14th and 16th, resulting in a net loss of sediment of 1.87 m³/m (Fig. 7). In contrast, between the 16th and 18th, there was a net gain of sediment over the same distance of 5.34 m³/m. The overall sediment balance for the storm event in the inner nearshore zone event was positive (Fig. 8). However, considering the complete profile out to 180 m, there was actually a net loss of sediment of 2.11 m³/m. This erosion was the result of a dramatic loss of sediment from Bar 3 (both crest and trough), which occurred almost certainly during the latter half of the storm, when wave saturation reached lakeward of this bar. The crest of Bar 3 shifted almost vertically and moved offshore lower on the profile.

October 9th-October 16th

Much of sediment loss from the inner surf zone during this period resulted first from erosion of the beach step at 38 m; the depth of erosion reached almost 0.40 m, with much of this sediment was displaced landward to build a distinct berm on the beach face. There was also significant erosion of the crest and trough of Bar 2, and it was during this phase of net sediment loss from the inner surf zone that an incipient bar emerged through differential erosion of the shore terrace

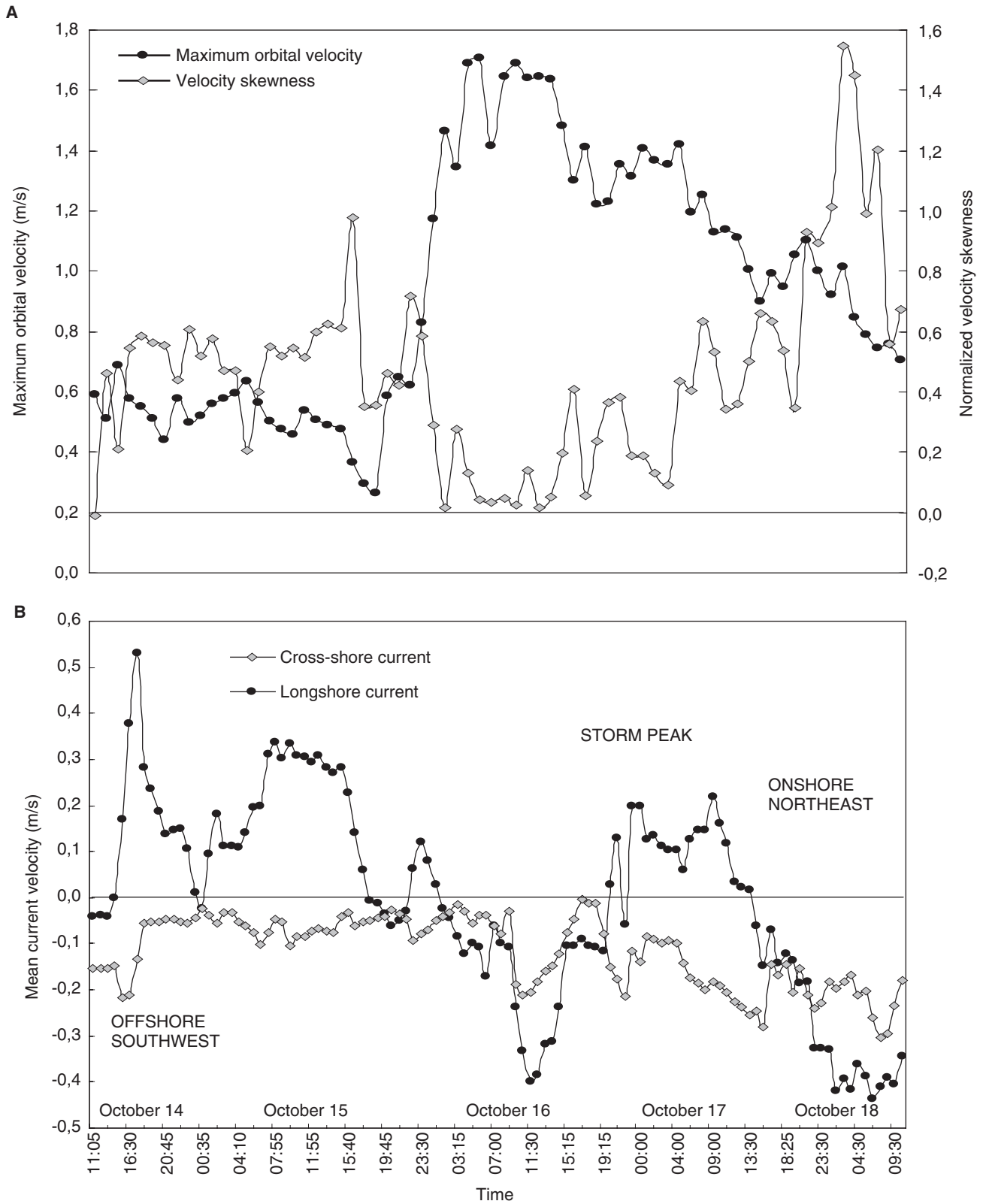

FIGURE 6. Time series of (A) the maximum cross-shore oscillatory (orbital) velocity (u_{max}) and oscillatory velocity skewness (u_{sk}); and (B) the cross-shore and longshore mean currents. All values recorded at station S2.

Séries temporelles de (A) la vitesse oscillatoire (orbitale) maximale de biais (u_{max}) et de son asymétrie (u_{sk}), et de (B) la vitesse des principaux courants et contre-courants. Toutes les valeurs ont été enregistrées à la station S2.

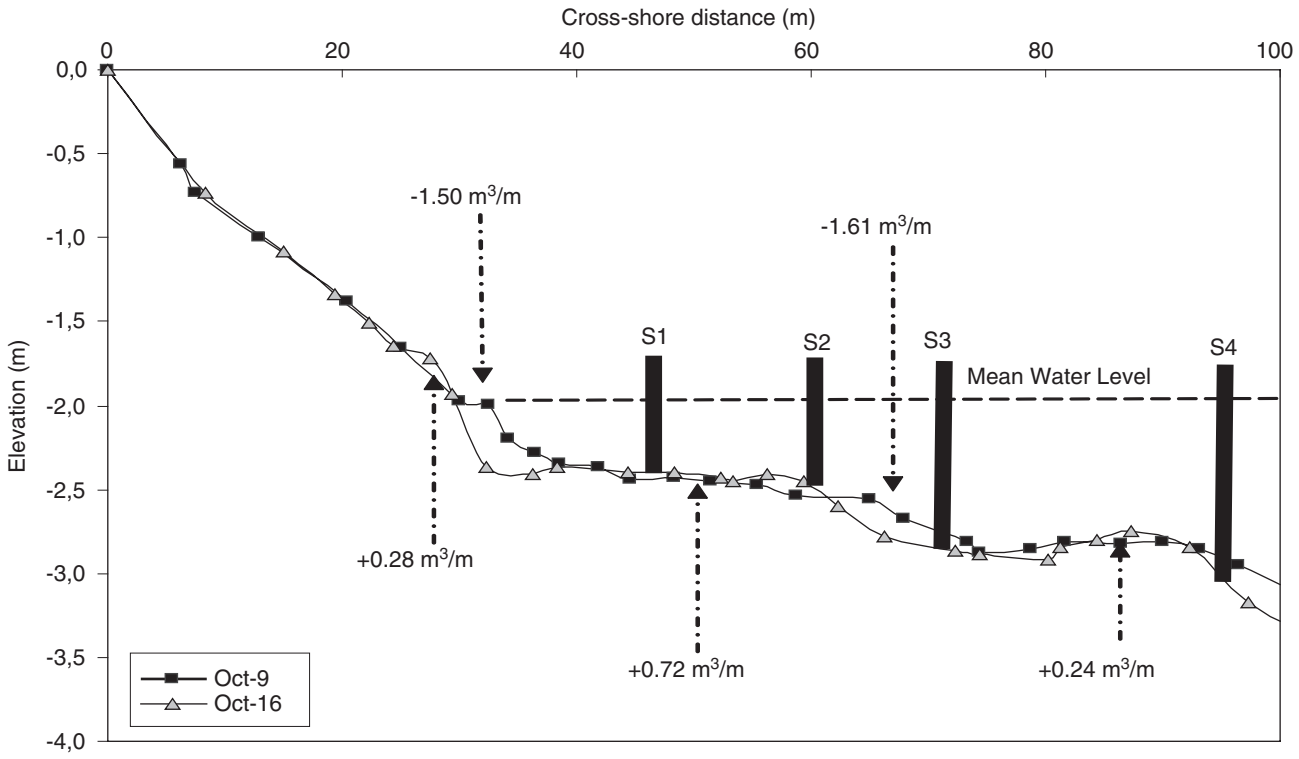

FIGURE 7. Nearshore topographic profiles along transect T3 at Burley Beach on October 9th and October 16th, 2001. Note: stations S2 and S4 are marked for reference and profile differences have been converted to volumetric measures (m^3/m of beach width).

Profil topographique de la côte le long du transect T3 à la plage de Burley le 9 octobre et le 16 octobre 2001. Note : les stations S2 et S4 sont les points de référence, et les différences entre les profils ont été converties en mesures volumétriques (en m^3/m de largeur de plage).

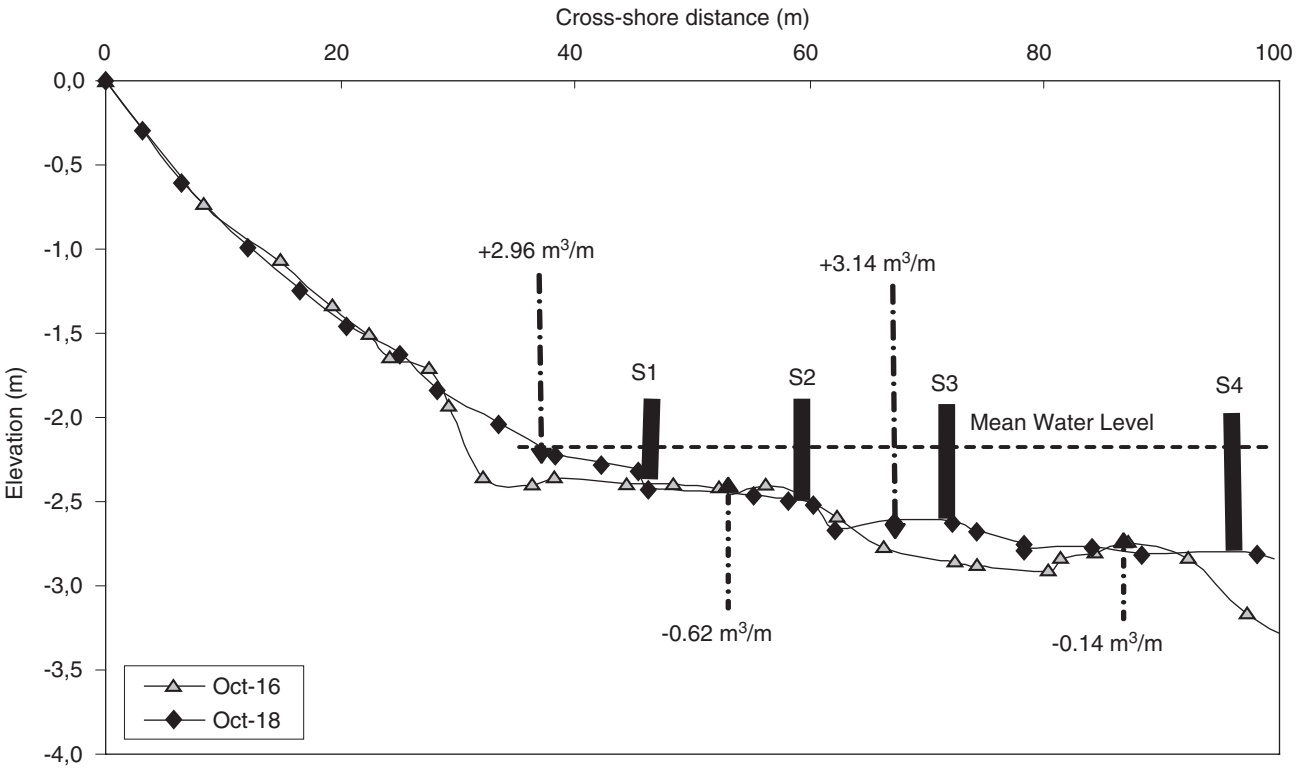

FIGURE 8. Nearshore topographic profiles along transect T3 at Burley Beach on October 16th and October 18th, 2001. Note: stations S2 and S4 are marked for reference and profile differences have been converted to volumetric measures (m^3/m of beach width).

Profil topographique de la côte le long du transect T3 à la plage de Burley le 16 octobre et le 18 octobre 2001. Note : les stations S2 et S4 sont les points de référence, et les différences entre les profils ont été converties en mesures volumétriques (en m^3/m de largeur de plage).

(Fig. 7). Accretion at station S2 and landward to 38 m, coupled with erosion at station S3, produced an incipient crest, located at 55 m. However, the bar was still somewhat irregular in form, suggesting that when wave energies decayed on the afternoon of the 16th, the bar had not completely formed.

October 16th-October 18th

During the most intense part of the storm, further morphological change occurred: (a) the incipient bar-trough system in the inner surf zone increased in relative relief, assumed the more characteristic strongly asymmetric form, typical of a second bar, with steeper lakeward slope. Its crest was also displaced 16 m lakeward over a period of 40 h, at an average migration rate of 0.40 m/h; this was significantly less than the 2.5 m/h recorded in 1992 for the migration of Bar 2 (Aagaard and Greenwood, 1995a). (b) A new beach step and shore terrace was produced, which prograded lakeward as the new Bar 1 also migrated lakeward. The former was the result of significant accretion at the shoreline (2.96 m^3/m; Fig. 8). (c) Bar 2 also migrated 10 m offshore, primarily as a result of accretion on its lakeward slope; thus, the new Bar 1 and Bar 2 migrated in concert. (d) While the relative relief of Bar 3 did not change significantly, erosion of its trough and crest lowered the whole bar form in absolute terms (0.25 m), while at the same time it was displaced lakeward (6 m). This erosion accounted for most of the overall sediment loss from the upper shoreface profile that was noted in the earlier section. (e) The pattern of local accretion and erosion across the three bar system, coupled with the overall loss of sediment resulted in a steepening of the average nearshore slope.

SEDIMENT TRANSPORT AND THE ASSOCIATED HYDRODYNAMICS

The spatial and temporal patterns of accretion and erosion in the inner surf zone and the associated morphological response noted above, especially the emergence of an incipient bar and its further growth and migration, can best be explained by the cross-shore distribution of the storm-induced sediment flux. Station S2 was the fully instrumented transport station closest to the emergent bar within the inner surf zone and therefore the sediment flux rate measured throughout the storm at this position will be used to provide an explanation for the emergent bar morphodynamics.

CROSS-SHORE AND LONGSHORE SUSPENDED SEDIMENT TRANSPORT

Table I gives the cross-shore and the longshore suspended sediment transport rates recorded at station S2, averaged over the three nominal elevations (z = 0.05, 0.10, 0.15 m) and averaged over the complete storm. Ratios between the net transport rate (depth- and storm-averaged) and the gross transport rate are also given. A number of aspects deserve mention: (a) the average cross-shore transport rate was positive, indicating that the net transport was directed shoreward; the average longshore transport rate was negative indicating transport to the southwest. (b) The net transport rates in both the cross-shore and longshore directions were significantly smaller than the gross transport rates; in the cross-shore direction it was less than 50%, while in the longshore direction it was no more than 13% (Table I). Thus, while it was clear that a very large amount of wave energy was dissipated in setting suspended sediment in motion at station S2, only a part of this energy contributed to the net flux that produced erosion/accretion and the resultant morphological change. (c) In terms of the directionality of the net sediment flux, the cross-shore net transport rates were significantly larger than the alongshore transport rates. This was true even for transport by the mean currents, which because of the reversing nature of the longshore currents gave a relatively small net flux to the southwest. (d) The wave-induced oscillatory transport at all frequencies dominated the net cross-shore suspended sediment flux, while the mean current clearly dominated the longshore flux.

Figures 9, 10 and 11 illustrate the time-variation in the depth-averaged, cross-shore wave transport, cross-shore net mean current transport and net longshore transport over the storm. The net fluxes are shown, together with the individual components, including the oscillatory transport rate at various frequencies and transport by the mean current. Figures 12, 13 and 14 illustrate the vertical distribution of the net cross-shore transport rate as well as the individual transport components at station S2 at three different times in the storm: October 14th, 21:35; October 16th, 23:15; October 18th, 03:30.

A number of features characterize the cross-shore transport: (a) through the first half of the storm (October 14th, 11:05-October 16th, 19:15), the net transport rates remained ≤0.5 $kg/m^2/s$, but were relatively steady and directed onshore primarily by incident gravity waves, which accounted for 82% of the net oscillatory transport at this time. (b) Associated with the rapid increase in wave height late on October 16th, there was an automatic increase in both the near-bed oscillatory and mean currents. The net transport rates responded rapidly to this increase in wave energy and, as the storm peaked, reached a maximum hourly rate of +3.79 $kg/m^2/s$. (c) Although the net transport was directed shoreward, there was considerable

TABLE I

Transport rates at station S2, October 14th 18th, 2001

Transport Component	Cross-shore Transport ($kg/m^2/s$)	Alongshore Transport ($kg/m^2/s$)
Average net transport rate	0.73	-0.12
Average gross transport rate	1.70	0.93
Net:Gross Ratio (%)	~43%	~13%
Total net transport rate	-11.8	-12.34
Total gross transport rate	172	94
Net:Gross Ratio (%)	~7%	~13%
Average mean transport rate	-0.47	-0.13
Total mean transport rate		-13.00
Average net oscillatory transport rate	1.2	0.01
Total net oscillatory transport rate	120.80	0.66

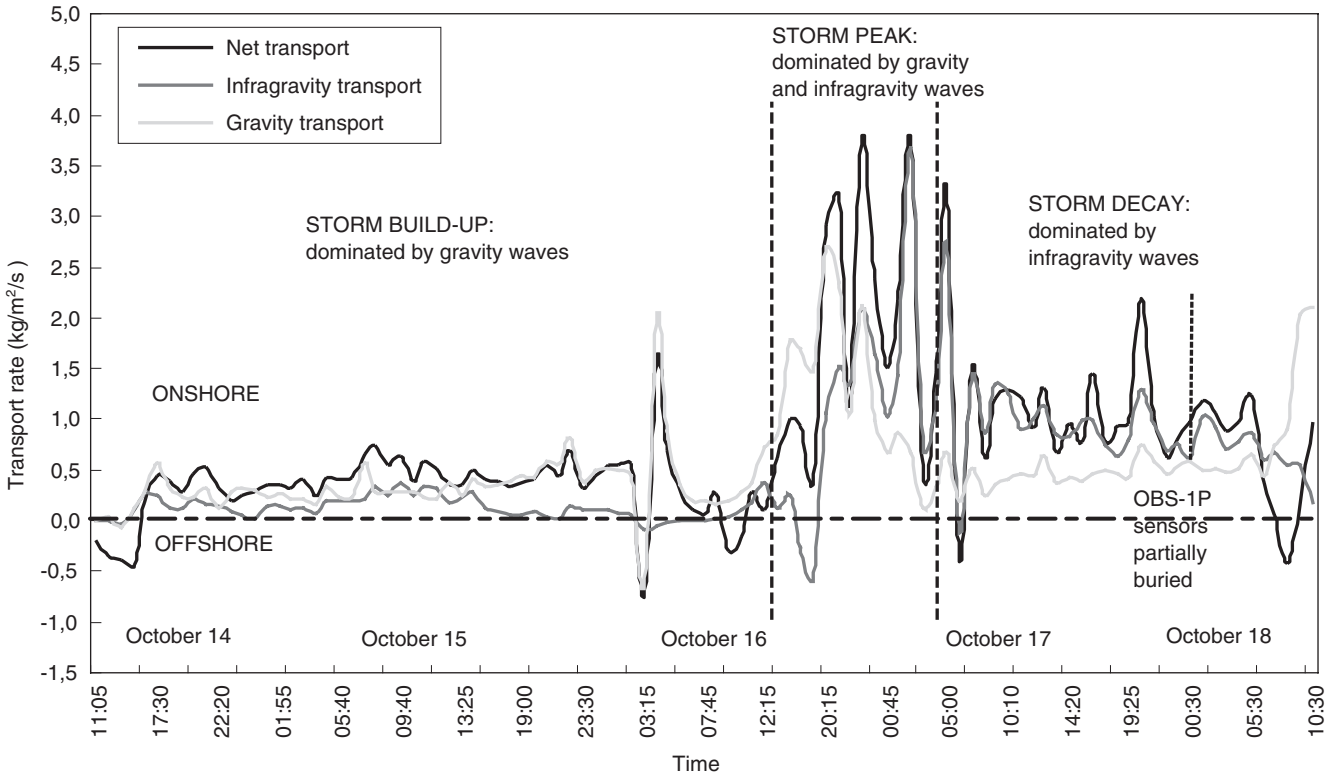

FIGURE 9. Hourly cross-shore suspended sediment transport rates recorded at station S2 for the period October 14th to 18th, 2001. The overall resultant net transport rate and the transport by gravity and infragravity waves are shown. Each data point represents the sum of the transport rates recorded at the three nominal elevations of z = 0.05, 0.10, and 0.15 m.

Taux horaires du transport en suspension de biais enregistrés à la station S2 pour la période du 14 au 18 octobre 2001. Le taux de transport net et le transport par les vagues de gravité et d'infragravité sont illustrés. Chaque point représente la somme des taux de transport aux élévations nominales de z = 0,05, 0,10 et 0,15 m.

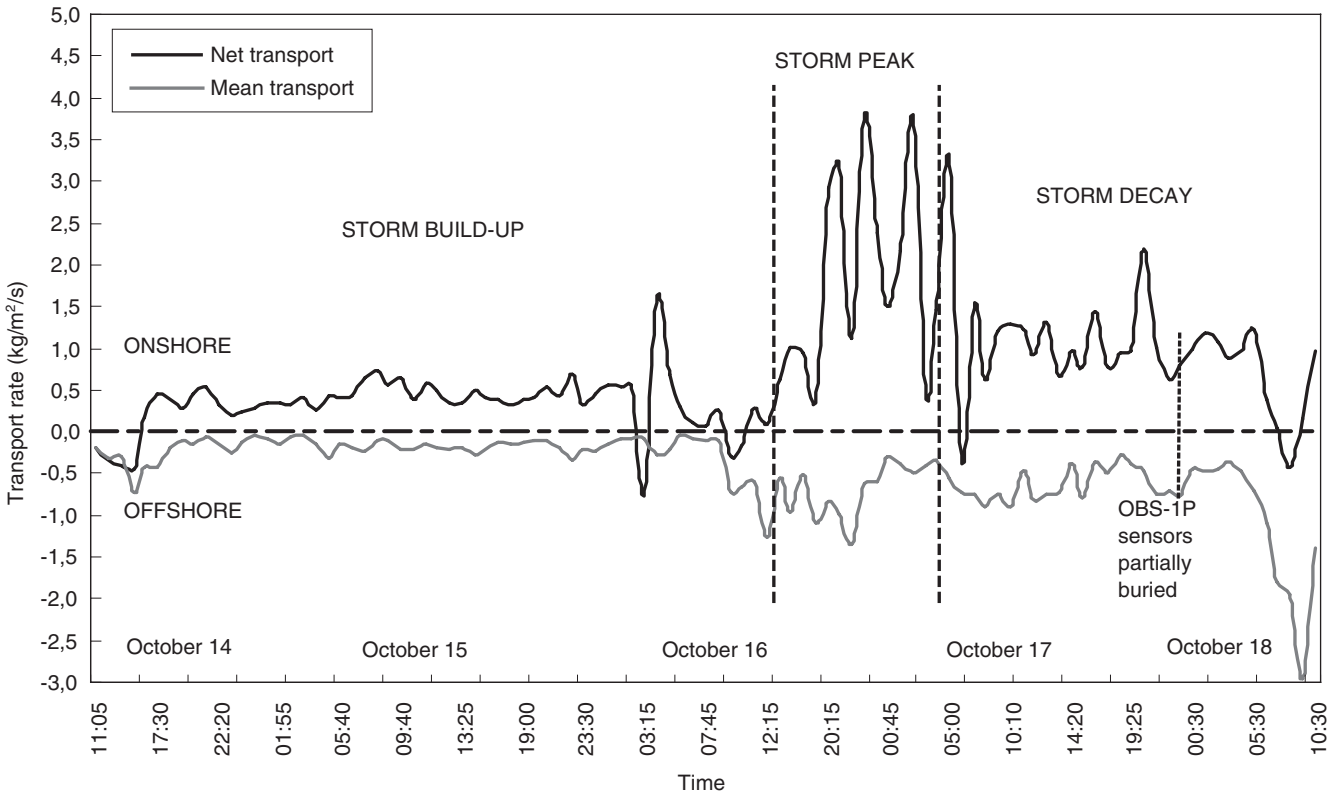

FIGURE 10. Hourly cross-shore suspended sediment transport rates recorded at station S2 for the period October 14th to 18th, 2001. The resultant net transport rate is shown as well as the transport by the cross-shore mean current.

Taux horaires du transport en suspension de biais enregistrés à la station S2 pour la période du 14 au 18 octobre 2001. Le taux de transport net est illustré, de même que le taux de transport par le contre-courant moyen.

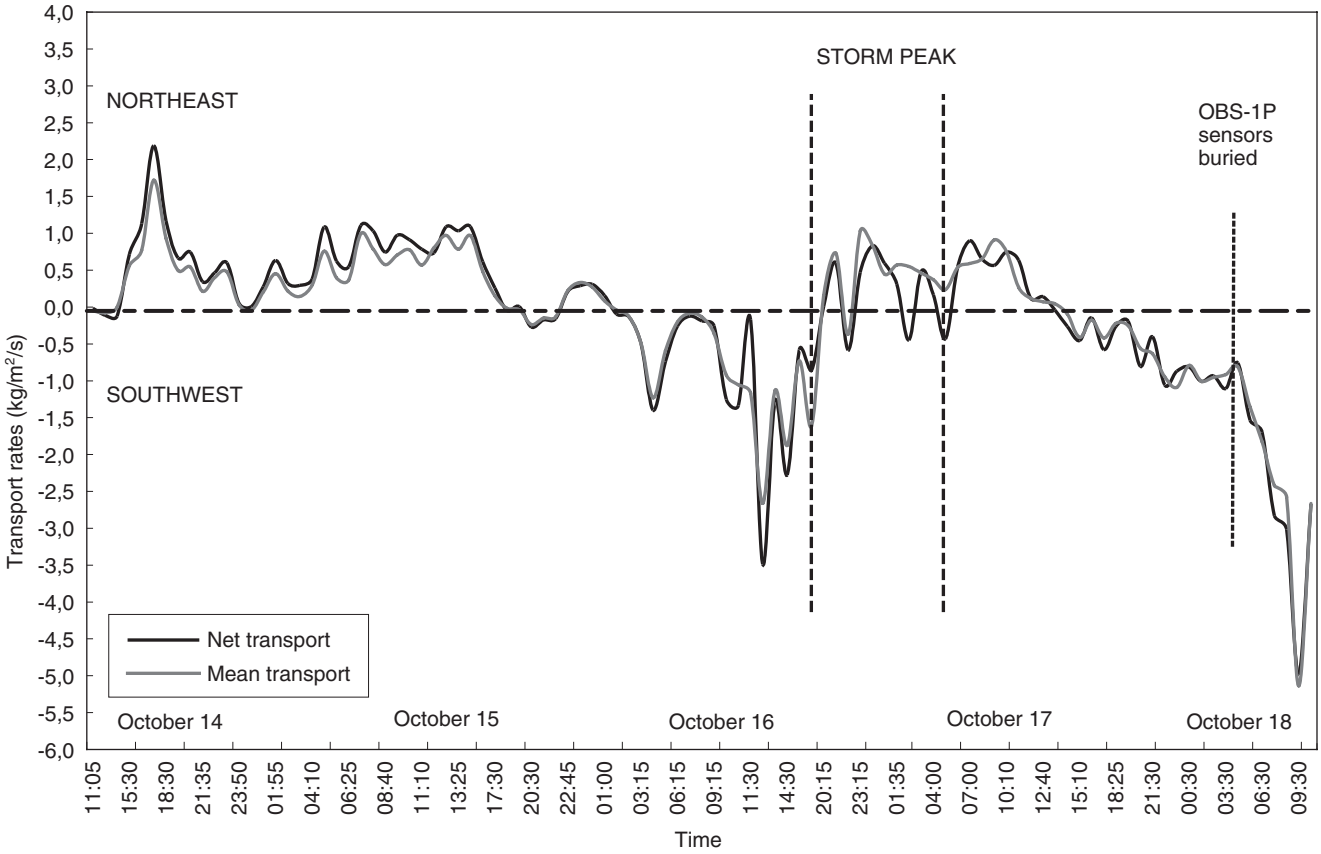

FIGURE 11. Hourly longshore suspended sediment transport rates recorded at station S2 for the period October 14th to 18th, 2001. The resultant net transport rate is shown as well as the mean transport rate by the longshore currents. The net and mean transport rates are essentially identical with only a small contribution from wave transport and this was at very low frequency.

Taux horaires du transport en suspension enregistrés à la station S2 pour la période du 14 au 18 octobre 2001. Le taux de transport net est illustré, de même que le taux de transport moyen par les courants. Les taux nets et moyens sont quasiment identiques, avec une légère contribution par le transport des vagues de très faible fréquence.

variability in the magnitudes at the storm peak (<0.5 to >3.7 kg m²/s). Examination of the near-bed currents and sediment concentrations indicate that the varying transport rates were a response to changes in the concentrations recorded by the optical sensors, not changes in the near-bed velocities (waves were saturated at this time at station S2). Such apparently rapid changes in concentration can be explained by changes in sensor elevation. The most likely scenario causing such rapid changes was the migration of large megaripples (see Aagaard *et al.*, 2001); these bedforms are ubiquitous during storms in these depths (unpublished data). When the sensors are positioned over the megaripple crest, recorded concentrations will be enhanced and when the sensors are positioned over the trough of the bedform, the measured concentrations decrease. (d) Although the incident gravity waves actually decreased slightly in height during the storm peak, as a result of initial wave breaking being displaced further and further lakeward, the maximum net transport rates still ranged between 2.19 and 3.79 kg/m²/s. However, at this time the infragravity (including far infragravity) frequencies dominated the suspension transport, accounting for 57% and 28% of the net SST rates respectively (Fig. 9). (e) Transport rates decreased relatively rapidly after the storm peak (around 07:00, October 17th), and remained relatively steady for the remainder of the storm (at 0.5-1 kg m²/s; Fig. 9). (f) With few exceptions, the cross-shore sediment flux was directed onshore throughout the storm event at station S2.

Examination of the sediment transport rates at station S2 at specific times during the storm reveal details of the wave frequencies and mean currents driving the suspension transport (Osborne and Greenwood, 1992). Figures 12, 13 and 14 illustrate the vertical distribution of the individual transport components at three different times in the storm: October 14th, 21:35; October 16th, 23:15; October 18th, 03:30. A feature common to most is the tendency for a decrease in net transport with height above the bed; because of the nature of oscillatory motion, sediment suspension under waves is extremely episodic (Greenwood *et al.*, 1991), and thus concentrations decrease dramatically with elevation. However, the decrease is dependent on frequency; the decrease is less at far infragravity than gravity wave frequencies. In contrast, transport by the cross-shore mean current (almost certainly undertow) is much more uniform within the bottom 0.15 m. Also, it is clear that the net transport was a much larger percentage of the gross transport at the storm peak (75%), than either during the first part of the storm or during the decay (30% and 15%

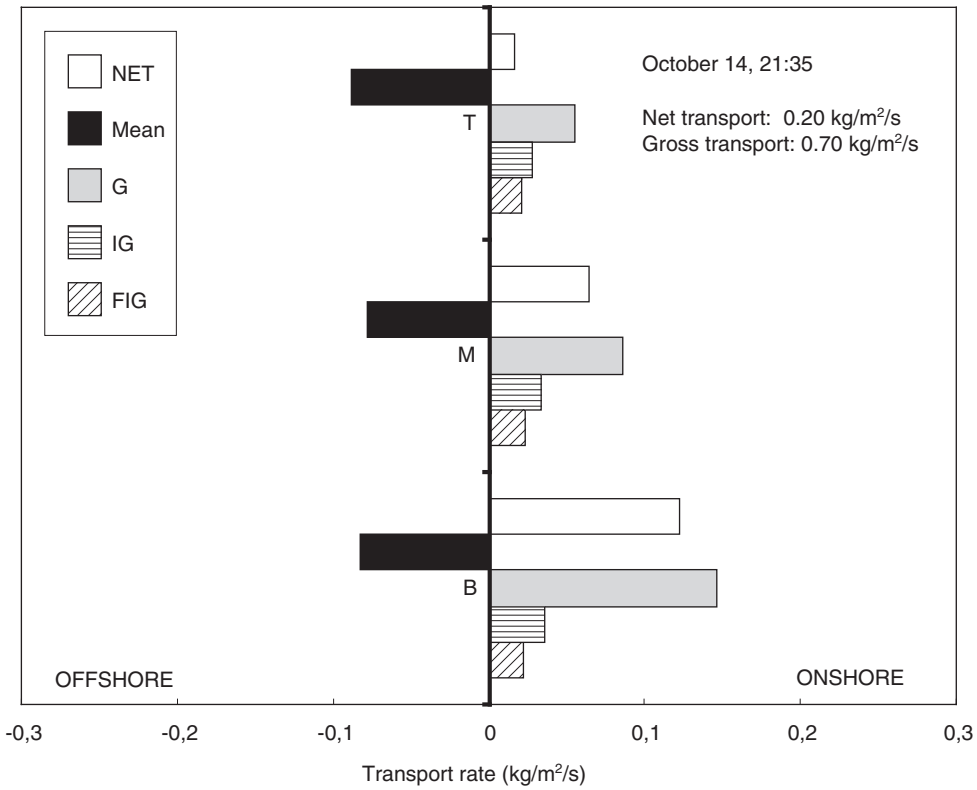

FIGURE 12. Contributions to the net cross-shore transport rate at 21:35, October 14th, from each individual transport mechanism: the mean current (Mean), gravity waves (G), infragravity waves (IG) and far infragravity waves (FIG). Transport rates at the three nominal elevations (z = 0.05, 0.10, 0.15 m) are illustrated, as are the onshore and offshore directions. Values for the overall net transport and gross transport rates are also given.

Contributions au taux de transport en biais net à 21h35, le 14 octobre, de chaque mécanisme de transport : courant moyen (moyen), vagues de gravité (G), vagues d'infragravité (IG) et vagues d'infragravité lointaines (FIG). Les taux de transport aux trois élévations nominales (z = 0,05, 0,10, 0,15 m) sont illustrés en fonction de la direction par rapport à la côte. Les valeurs du taux de transport global net et brut sont également livrées.

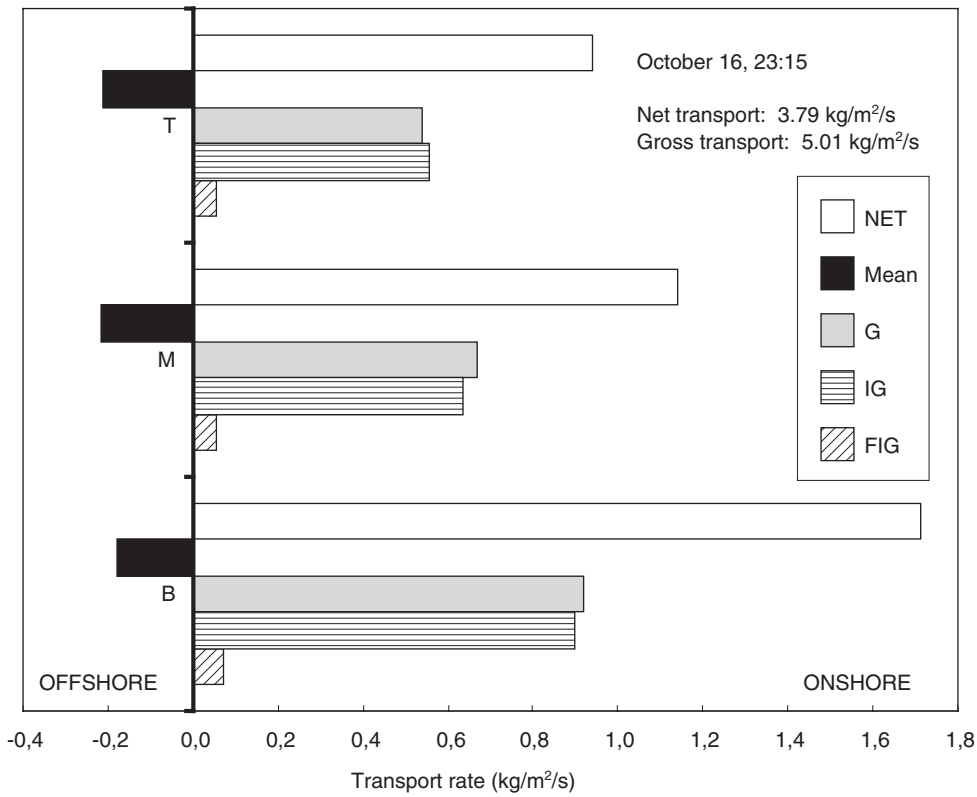

FIGURE 13. Contributions to the net cross-shore transport rate at 23:15, October 16th, from each individual transport mechanism: the mean current (Mean), gravity waves (G), infragravity waves (IG) and far infragravity waves (FIG). Transport rates at the three nominal elevations (z = 0.05, 0.10, 0.15 m) are illustrated, as are the onshore and offshore directions. Values for the overall net transport and gross transport rates are also given.

Contributions au taux de transport en biais net à 23h15, le 16 octobre, de chaque mécanisme de transport : courant moyen (moyen), vagues de gravité (G), vagues d'infragravité (IG) et vagues d'infragravité lointaines (FIG). Les taux de transport aux trois élévations nominales (z = 0,05, 0,10, 0,15 m) sont illustrés en fonction de la direction par rapport à la côte. Les valeurs du taux de transport global net et brut sont également livrées.

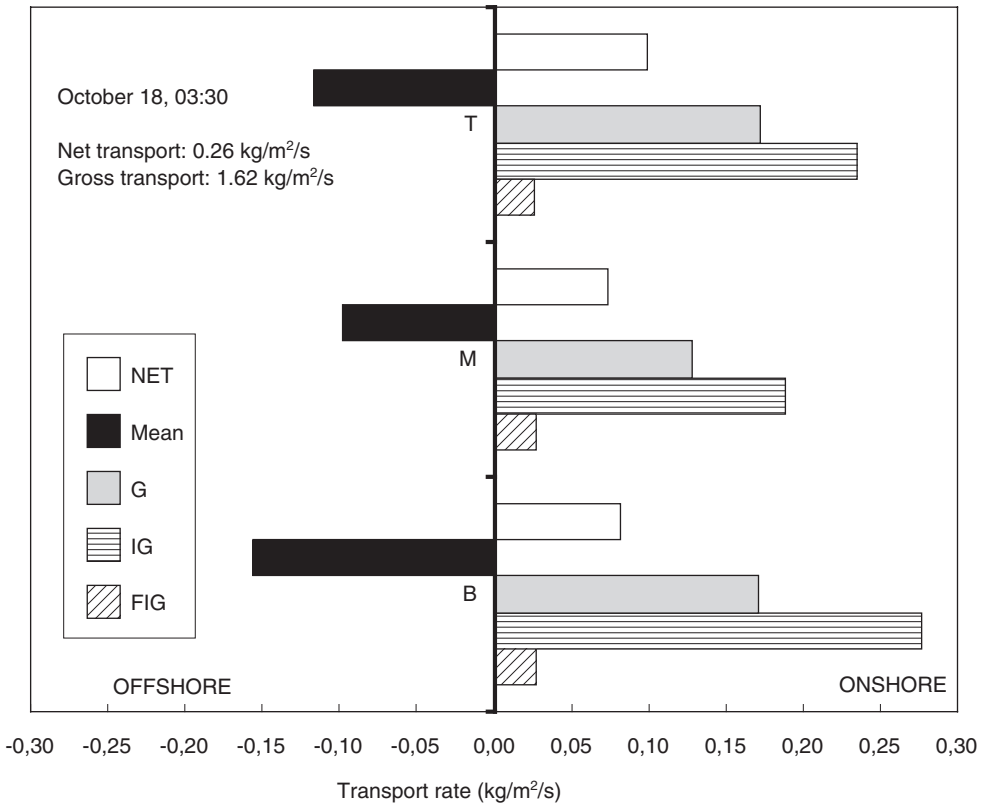

FIGURE 14. Contributions to the net cross-shore transport rate at 03:30, October 18th, from each individual transport mechanism: the mean current (Mean), gravity waves (G), infragravity waves (IG) and far infragravity waves (FIG). Transport rates at the three nominal elevations (z = 0.05, 0.10, 0.15 m) are illustrated, as are the onshore and offshore directions. Values for the overall net transport and gross transport rates are also given.

Contributions au taux de transport en biais net à 03h30, le 18 octobre, de chaque mécanisme de transport : courant moyen (moyen), vagues de gravité (G), vagues d'infragravité (IG) et vagues d'infragravité lointaines (FIG). Les taux de transport aux trois élévations nominales (z = 0,05, 0,10, 0,15 m) sont illustrés en fonction de la direction par rapport à la côte. Les valeurs du taux de transport global net et brut sont également livrées.

respectively). With respect to the sediment balance, the resultant net transport was essentially directed shoreward at all elevations and at each stage of the storm and, indeed, throughout the storm. Also, the net oscillatory transport was directed shoreward at all frequencies and again at all three elevations monitored. In contrast, the transport induced by the time-averaged mean current, which reached a maximum of 0.29 m/s at station S2 during the storm peak and early decay phases, was always directed offshore. A six-hour long data record (01:45-07:45, October 16th) gave an average net onshore transport rate of +1.28 kg/m²/s. The oscillatory transport was clearly dominant and the resultant hourly average net cross-shore transport at station S2 throughout the event was +0.73 kg/m²/s (see Table I), with hourly maxima up to +3.79 kg/m²/s. Thus the net gain of sediment in the inner nearshore noted above can clearly be related to the dominance of the wave-induced sediment flux.

With respect to the relevant frequencies that contributed to the oscillatory transport, the incident gravity waves (<0.05 Hz, 20 s) were dominant in the first half of the storm, when breaking was restricted to the inner near shore zone. At the storm peak, when suspension transport also peaked, the resultant net cross-shore transport rates at station S2 were on average 87% larger than rates during the first half of the storm. Also at this time, infragravity waves were at least as important, or on occasion more important, than the gravity waves; during the decay phase of the storm it was clear that the infragravity frequencies dominated the oscillatory transport regime (Figs. 9, 14, 15). Thus, there was also a distinct lag in the infragravity wave transport compared to the gravity wave transport. Certainly, infragravity energies became dominant in the wave and current spectra in a manner similar to the lag that had previously been noted by Bauer and Greenwood (1990) in a barred system in Georgian Bay (an arm of Lake Huron).

It is clear that the large landward flux of sediment was not simply advected alongshore by the longshore current, either to the NE or SW, even though these currents reached maxima of 0.55 and 0.44 m/s respectively at station S2. The accretion in the inner surf zone can therefore be attributed to this landward flux.

As the storm began to decay on October 17th around 06:00, a distinct stratification in the SST occurred at station S2. In the lower water column (z = 0.05 and 0.10 m) the SST was directed offshore, while at z = 0.15 m the SST was still directed shoreward. The offshore flux near the bed was dominated by the infragravity wave component, while the mean current (undertow) played a smaller role; the co-spectrum exhibited a large, statistically significant peak at 0.017 Hz (59 s); transport at incident wave frequencies was negligible at this time.

As the storm-waves decayed over the next twelve hours, the net cross-shore transport decreased dramatically, although the gross transport rates remained large. Analysis of a 12-hour long record (October 17th, 20:30-October 18th, 07:30) yielded an average net suspended sediment transport rate of only +0.16 kg/m²/s, while the gross transport rate was 2.69 kg/m²/s. However, the net transport was still directed shoreward at station S2. Offshore transport by the mean current was large at all elevations indicating the re-establishment of undertow at S2;

however, this transport was more than balanced by the onshore flux by the oscillatory components. Transport at infragravity and far infragravity frequencies actually dominated the landward transport at this stage, accounting for 50% of the net oscillatory transport. The cospectrum revealed peaks at a range of infragravity frequencies up to 0.007 Hz (143 s) with a marked peak frequency at 0.014 Hz (72 s; Fig. 15). However, in this unusually long time series, a significant peak also occurred at far infragravity frequencies (0.001 Hz, 17 min). Cross-shore transport at such a low frequency has been ascribed to shear waves (Aagaard and Greenwood, 1995b; Miles *et al.*, 2002), which is also the most likely mechanism in this instance, since the longshore transport rates over this time period also revealed a strong signal at this frequency.

During the final hours of the event, the net shoreward SST decreased to zero and actually reversed for one sampling period, as a result of the dominance of the undertow (Figs. 9-10). However, the optical sensors recorded extremely large sediment concentrations at this time as a result of bar accretion at station S2 as the bar was developing; this decreased the relative elevation of the sensors and partially buried the array.

LONGSHORE SUSPENDED SEDIMENT TRANSPORT

As expected, the mean current dominated the longshore suspended sediment transport rates, with waves (essentially only the infragravity and far infragravity frequencies) making only a negligible contribution (Table I). On October 14th and 15th with the approach of the sharp cold front, sediment was transported initially to the northeast by longshore currents, generated by winds and waves out of the southwest (Fig. 3). As the winds shifted rapidly to the west and northwest (Fig. 3) with the frontal passage, the waves and currents shifted also; longshore currents up to 0.44 m/s towards the southwest were generated at station S4. However, at the peak of the wave activity, the longshore transport rates were actually not significantly different from earlier in the storm. In general, the net longshore transport rates were of the same order of magnitude as the net cross-shore transport rates, except for the 10 h period around the storm peak when the cross-shore transport rates were larger by a factor of 4. Although the net longshore transport rates reached 2.3 kg/m^2/s to the northeast and 3.5 kg/m^2/s to the southwest, over the entire storm there was only a small net balance and this was in favour of the southwest direction at a rate of 0.12 kg/m^2/s at station S2 (Fig. 11; Table I). There was some evidence for longshore transport at far infragravity frequencies (0.004 Hz, 4.2 min; 0.006 Hz, 2.8 min). These very low frequencies may indicate shear wave activity, which is relatively common where steady longshore currents develop (Aagaard and Greenwood, 1995b). These frequency bands accounted for approximately half of the net oscillatory transport rate, although the oscillatory transport as a whole was negligible compared to the transport by the mean current.

DISCUSSION AND CONCLUSIONS

The upper shoreface at Burley Beach in southeastern Lake Huron is always characterized by a multi-bar system. Two to three subaqueous bars, often with a subaerial swash ridge or berm are always present in some combination. This can be considered to be the long-term equilibrium morphology. However, the bars are dynamic; they form, migrate and disappear over a bar cycle which may take years to complete (see

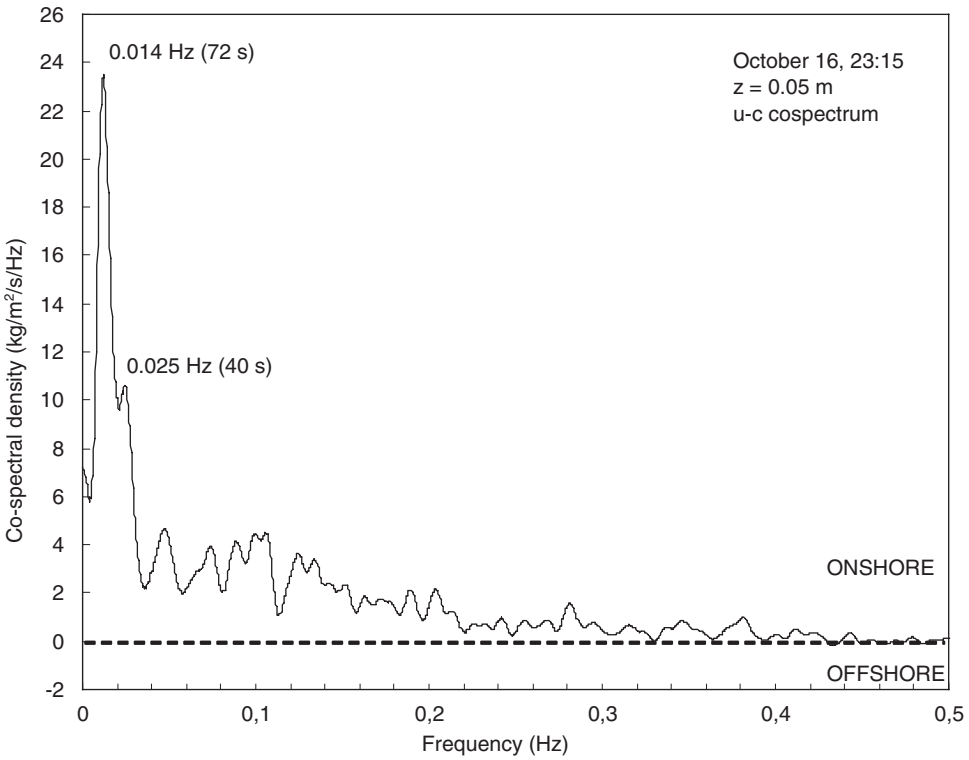

FIGURE 15. Cospectrum of cross-shore velocity and suspended sediment concentration measured at station S2 at 23:15 on October 16th. Note: (a) the lack of variance at incident wave frequencies (0.13-0.17 Hz) indicates no coherent transport by the incident waves; (b) the large statistically significant peak in variance at 0.014 Hz indicates significant transport by infragravity waves.

Spectre combiné de la vitesse en biais et de la concentration des sédiments en suspension mesurées à la station S2 à 23h15, le 16 octobre. Note: (a) la faible variance de la fréquence des vagues d'incidence (0,13-0,17 Hz) indique un transport non cohérent et (b) le point se produisant à 0,014 Hz indique un transport significatif par les vagues d'infragravité.

Wijnberg, 1995; Houser and Greenwood, 2005). It has been demonstrated that differential erosion of a nearshore terrace initiated the emergence of an incipient bar; it continued to grow in relative relief and migrated significantly in the offshore direction all within a single, though complex, storm event. With respect to bar emergence this study indicates that: (a) the new bar emerged within the inner surf zone close to the shoreline, initially as an irregular trough-crest form, from differential erosion of a sub-horizontal shore terrace; (b) the emergent bar increased in relative relief by both erosion of the trough and accretion on the crest, and the form became more typically asymmetric as incident wave energy increased within the inner surf zone; (c) bar growth was also associated with a significant lakeward displacement (offshore migration) of the bar into deeper water. At this time the beach step also prograded significantly resulting in a new shore terrace; consequently the bars lakeward of the emerging bar were also displaced lakeward to provide the necessary accommodation space.

The initial emergence of the new bar was characterized by an overall negative sediment balance in the inner surf zone (-1.87 m^3/m), while subsequent increases in bar relief, and development of a more regular asymmetrical form, were associated with a large positive sediment balance (+5.34 m^3/m). Over the whole storm, the inner surf zone was characterized by positive sediment balance +3.20 m^3/m. Thus, the bar was initiated in a situation of net sediment loss, as the shore terrace was eroded, but its growth and migration occurred in the presence of a large positive sediment budget. While the mean cross-shore currents in the inner surf zone always transported sediment offshore, this was more than balanced by onshore transport, first primarily by the incident gravity waves and subsequently (at the storm peak and into the decay period) by oscillatory transport at infragravity frequencies.

The longshore transport was clearly significant in terms of the total transport; however, with sediment transported both to the NE and subsequently to the SW as the wave field switched, the net resultant was a relatively small resultant transport to the SW. Although the storm resulted in a net transport to the SW, the historical pattern of littoral drift, this transport did not influence bar initiation, although it may have supplied sediment for bar growth. The primary mechanism for bar initiation and subsequent growth was the cross-shore displacement of sediment by wave-driven (oscillatory) transport and cross-shore mean currents.

ACKNOWLEDGEMENTS

Funding was provided by operating and equipment grants from the Natural Sciences and Engineering Research Council of Canada (NSERC) awarded to B. Greenwood. A Postgraduate Scholarship from the same body is acknowledged by C. Houser. We would like to thank Mike Doughty, Trisha Ralph, Sarah Taylor, and Thera Ip for invaluable assistance both in the field and the laboratory. This paper evolved from the M.Sc. thesis of A. Permanand-Schwartz carried out under the supervision of B. Greenwood and is a contribution from the Canadian Coastal Sediment Transport Programme (C-COAST). We also thank the Ontario Ministry of Natural Resources for permission to carry out research in Pinery Provincial Park, Ontario, and Mary-Louise Byrne, Alex Aitken and Alan Trenhaile for their very helpful reviews.

REFERENCES

Aagaard, T., Greenwood, B. and Nielsen, J., 2001. Bed level changes and megaripple migration on a barred beach. Journal of Coastal Research, Special Issue 34, p. 110-116.

Aagaard, T. and Greenwood, B., 1994. Suspended sediment transport and the role of infragravity waves in a barred surf zone. Marine Geology, 118: 23-48.

Aagaard, T. and Greenwood, B., 1995a. Suspended sediment transport and morphological response on a dissipative beach. Continental Shelf Research, 15: 1061-1086.

Aagaard, T. and Greenwood, B., 1995b. Longshore and cross-shore suspended sediment transport at far infragravity frequencies in a barred environment. Continental Shelf Research, 15: 1235-1249.

Aagaard, T. and Greenwood, B., 1999. Directionality of cross-shore sediment transport in the surf zone under high-energy conditions. Coastal Sediments '99, American Society of Civil Engineers, New York, 16 p.

Andrews, E., 1870. The North American Lakes considered as Chronometers of Post Glacial Time. Transactions of the Chicago Academy of Sciences, No. 2, p. 14.

Angel, J.R. and Isard, S.A., 1997. An observational study of the influence of the Great Lakes on the speed and intensity of passing cyclones. Monthly Weather Review, 125: 2228-2237.

Bauer, B.O. and Greenwood, B., 1990. Modification of a linear bar-trough system by a standing edge wave. Marine Geology, 92: 177-204.

Carter, R.W.G., 1988. Coastal Environments: an introduction to the physical, ecological and cultural systems of coastlines. Academic Press, London, 617 p.

Cooper, A.J., 1976. Quaternary Geology of the Grand Bend–Parkhill Area, Southern Ontario. Ontario Division of Mines, Sudbury, OFR5215, 119 p.

Davidson-Arnott, R.G.D., 1988. Controls on formation of barred nearshore profiles. Geographical Review, 78: 185-193.

Davidson-Arnott, R.G.D. and McDonald, R.A., 1980. Morphology and sedimentology of multiple bar systems, southern Georgian Bay, Ontario, p. 417-428. *In* S.B. McCann, ed., The Coastline of Canada. Geological Survey of Canada, Ottawa, Paper 80-10.

Davis, R.A., Jr. and Fox, W.T., 1972a. Coastal processes and nearshore sand bars. Journal of Sedimentary Petrology, 42: 401-412.

Davis, R.A., Jr. and Fox, W.T., 1972b. Four-dimensional model for beach and nearshore sedimentation. Journal of Geology, 80: 484-493.

Desor, E., 1851. Report of the Lake Superior Land District, Part II. Edited by J.W. Foster and J.D. Whitney. United States General Land Office, 1866, 258 p.

Dubois, R.N., 1973. Seasonal variation of a limnic beach. Geological Society of America Bulletin, 84: 1817-1824.

Evans, O.F., 1940. The low and ball of the east shore of Lake Michigan. Journal of Geology, 48: 467-511.

Gilbert, G.K., 1885. The topographic features of lake shores. United States Geological Survey, Reston, 5th Annual Report, 111 p.

Gillie, R.D., 1974. The nearshore morphology of sand beaches on the Great Lakes shoreline of Southern Ontario. Unpublished M.Sc. Thesis, McMaster University, 140 p.

Gillie, R.D., 1980. Barred nearshore profiles in Great Lakes research. Proceedings of the Canadian Coastal Conference, 14 p.

Greenwood, B., 2003. Bars (Littoral), p. 40-43. *In* G.V. Middleton, ed., Encyclopaedia of Sedimentology. Kluwer Academic Publishers, Amsterdam.

Greenwood, B., 2004. Bars, p. 120-129. *In* M. Schwartz, ed., Encyclopaedia of Coastal Science. Kluwer Academic Publishers, Amsterdam.

Greenwood, B., Osborne, P.D., Bowen, A.J., Hazen, D.G. and Hay, A.E., 1991. Nearshore sediment flux and bottom boundary dynamics: the Canadian Coastal Sediment Transport Programme (C-COAST). *In* Proceedings of the 22nd International Conference of Coastal Engineering, Delft, Netherlands. American Society of Civil Engineers, New York, 14 p.

Greenwood, B., 1987. Sediment balance and bar morphodynamics in a multiple bar system, Georgian Bay, Canada, p. 1119-1143. *In* V. Gardiner, ed., International Geomorphology. John Wiley and Sons, London.

Greenwood, B. and Mittler, P.R., 1979. Structural indices of sediment transport in a straight wave-formed nearshore bar. Marine Geology, 32: 191-203.

Greenwood, B. and Mittler, P.R., 1984. Sediment flux and equilibrium slopes in a barred nearshore. Marine Geology, 60: 79-98.

Greenwood, B. and Davidson-Arnott, R.G.D., 1975. Marine bars and nearshore sedimentary processes, Kouchibouguac Bay, New Brunswick, Canada, p. 123-150. *In* J. Hails and A. Carr, eds., Nearshore Sediment Dynamics and Sedimentation. John Wiley and Sons, London.

Greenwood, B. and Davidson-Arnott, R.G.D., 1979. Sedimentation and equilibrium in wave-formed bars: A review and case study. Canadian Journal of Earth Sciences, 16: 313-332.

Hale, P.B. and McCann, S.B., 1982. Rhythmic topography in a mesotidal low-wave-energy environment. Journal of Sedimentary Petrology, 52: 415-429.

Hands, E.H., 1976. Observations of barred coastal profiles under the influence of rising water levels, Eastern Lake Michigan, 1967-71. United States Army Corps of Engineers, Coastal Engineering Research Center, Technical Report 76-1, 113 p.

Houser, C.A., 2004. Feedback mechanisms in the morphodynamics of multiple barred nearshores. Unpublished Ph.D. Thesis, University of Toronto, 217 p.

Houser, C. and Greenwood, B., 2005. Profile response of a lacustrine multiple barred nearshore to a sequence of storm events. Geomorphology, 69: 118-137.

Inman, D.L., Elwany, M.H.S. and Jenkins, S.A., 1993. Shorerise and bar-berm profiles on ocean beaches. Journal of Geophysical Research, 98: 18181-18199.

Isard, S.A., Angel, J.R. and Van Dyke, G.T., 2000. Zones of origin for Great Lakes cyclones in North America, 1899-1996. Monthly Weather Review, 128: 474-485.

Keranen, R., 1985. Wave-induced sandy shore formations and processes in Lek Oulujarvi, Finland. Nordia, 19: 1-58.

Keulegan, G.H., 1948. An experimental study of submarine sand bars. Beach Erosion Board, Technical Report 3, 40 p.

Kindle, E.M., 1936. Notes on shallow water structures. Journal of Geology, 44: 863-867.

King, C.A.M., 1972. Beaches and Coasts. Edward Arnold, London, 470 p.

Lippmann, T.L. and Holman, R.A., 1990. The spatial and temporal variability of sand bar morphology. Journal of Geophysical Research, 95: 11575-11590.

Lippmann, T.L., Holman, R.A. and Hathaway, K.K., 1993. Episodic non-stationary behaviour of a two sand bar system at Duck, NC, USA. Journal of Coastal Research, Special Issue 15: 49-75.

Lowe, R.L., 1989. Continuous bedload sampling, p. 91-93. *In* R.J. Seymour, ed., Nearshore Sediment Transport. Plenum Press, New York, 418 p.

Miles, J.R., Russell, P.E., Ruessink, B.G. and Huntley, D.A., 2002. Field observations of the effect of shear waves on sediment suspension and transport. Continental Shelf Research, 22: 657-681.

Miller, R.L., 1976. Role of vortices in surf zone prediction: sedimentation and wave forces, p. 92-114. *In* R.A. Davis, Jr. and R.L. Ethington, eds., Beach and Nearshore Sedimentation. Society of Economic Paleontologists and Mineralogists, Tulsa, Special Publication 24.

Osborne, P.D. and Greenwood, B. 1992. Frequency dependent cross-shore suspended sediment transport 2: a barred shoreface, Bluewater Beach, Ontario, Canada. Marine Geology, 106: 25-51.

Owens, E.H., 1977. Temporal variations in beach and nearshore dynamics. Journal of Sedimentary Petrology, 47: 168-190.

Permanand-Schwartz, A., 2003. Hydrodynamics, suspended sediment transport and morphodynamics associated with a nearshore bar, Burley Beach, Ontario, Canada. Unpublished M.Sc. Thesis, University of Toronto, 189 p.

Ruessink, B.G. and Terwindt, J.H.J., 2000. The behaviour of nearshore sand bars on a timescale of years: a conceptual model. Marine Geology, 163: 289-302.

Russell, I.C., 1885. Geological history of Lake Lahontan. United States Geological Survey, Reston, Monograph II, p. 92-93.

Saylor, J.H. and Hands, E.B., 1970. Properties of longshore bars in the Great Lakes. *In* Proceedings of the 12th International Coastal Engineering Conference. American Society of Civil Engineers, New York, 15 p.

Shand, R.D., 2003. Relationships between episodes of bar switching, cross-shore bar migration and outer bar degeneration at Wanganui, New Zealand. Journal of Coastal Research, 19: 157-170.

Shepard, F.P., 1950. Longshore bars and longshore troughs. United States Army Corps of Engineers, Beach Erosion Board Technical Memorandum 15, 32 p.

Southgate, H.N. and Möller, I., 2000. Fractal properties of coastal profile evolution at Duck, North Carolina. Journal of Geophysical Research, 105: 11489-11507.

Sternberg, R.W., Shi, N.C. and Downing, J.P., 1989. Suspended sediment measurements. Continuous measurements of suspended sediment, p. 231-257. *In* R.J. Seymour, ed., Nearshore Sediment Transport. Plenum Press, New York, 418 p.

Thornton, E.B., Humiston, R.T. and Birkemeier, W., 1996. Bar/trough generation on a natural beach. Journal of Geophysical Research, 101: 12097-12110.

Whittlesey, C., 1896. Freshwater glacial drift of the northwestern States. Smithsonian Contribution 197, p. 17.

Wijnberg, K.M., 1995. Morphologic Behaviour of a Barred Coast over a Period of Decades. Ph.D. Thesis, Proefschrift Universiteit Utrecht, 245 p.

Wijnberg, K.M. and Kroon, A., 2002. Barred beaches. Geomorphology, 48: 103-120.

Wright, L.D., Chappell, J., Thom, B.G., Bradshaw, M.P. and Cowell, P., 1979. Morphodynamics of reflective and dissipative beach and inshore systems, southern Australia. Marine Geology, 32: 105-140.

Wright, L.D. and Short, A.D., 1984. Morphodynamic variability of surf zones and beaches: a synthesis. Marine Geology, 56: 93-118.

Zenkovitch, V.P., 1967. Processes of Coastal Development. Oliver and Boyd, London, 738 p.